QUANTUM
INFORMATICS

On-Demand Reconstruction of the Waveform of a Mössbauer Gamma-Ray Photon by Means of Delayed Acoustically Induced Transparency

I. R. Khairulin[a],* and Y. V. Radeonychev[a]

*[a] Gaponov-Grekhov Institute of Applied Physics, Russian Academy of Sciences,
Nizhny Novgorod, 603950 Russia*
*e-mail: khairulinir@ipfran.ru

A method has been proposed to reconstruct at arbitrary time the spectral–temporal characteristics of a 14.4-keV single-photon wave packet that is emitted by a ^{57}Co source and is resonantly absorbed in the medium of ^{57}Fe nuclei. The method is based on the frequency separation of the field emitted by the source and resonance nuclear polarization induced by this field by means of delayed acoustically induced transparency of the absorber, which appears after the activation of oscillations of the absorber at the corresponding frequency and amplitude. The proposed method has been compared to the known quantum-optical memory methods and methods of nuclear polarization control in the gamma-ray range. Experimental conditions have been proposed to implement the method. It has been shown that this method allows the implementation of the time-resolved Mössbauer spectroscopy of various media.

1. INTRODUCTION

One of the main requirements for the time-resolved diagnostics of materials, as well as for the transmission and procession of quantum information, is the determinancy of times when photons appear at certain points of space, including the possibility of controlling these times. This requirement can be satisfied by means of delay lines due to change in the path length or the propagation velocity of photons in a transparent medium, as well as by means of quantum memory, i.e., the localization of the electromagnetic field energy in the quantum state of the medium and the subsequent on-demand inverse transform of this state to a certain state of the electromagnetic field.

Numerous methods were proposed and implemented to delay photons by reducing the velocity of their propagation in a transparent medium in the optical range (see [1–16] and references therein). Electromagnetically induced transparency [17, 18] is one of the prevailing concepts in this field. Similar to electromagnetically induced transparency, the temporal [1–11] or spatial [12–16] dispersion of the medium is used to delay photons in most methods by creating a sharp dependence of the refractive index on the frequency or wave vector in the induced spectral transparency window of the medium, which covers the spectrum of the incident pulse. In addition to the implementation of electromagnetically induced transparency in various media, optical transparency was created by means of coherent population oscillations [6, 7], Autler–Townes splitting [10, 11], as well as in structured optomechanical systems [8, 9], optical waveguides [13, 14], and metastructures [15, 16].

Electromagnetically induced transparency and the related methods for delaying photons listed above are also used to implement quantum memory whose main advantage is the possibility to dynamically control the photon delay time [19–22]. A number of implemented quantum-optical memory methods for single photons based on nonresonant Raman scattering [23–25], atomic frequency comb [26–28], and various photon echo variants [29–35] are also promising.

The search for possibilities of the delay and storage of hard X-ray or soft gamma-ray photons (with energies from several to several tens of keV) in atomic nuclei is a promising field of quantum optics due to a number of unique properties of both these photons and resonant nuclear transitions [36, 37]. However, the above delay and quantum memory methods for optical photons are inefficient or unimplementable for gamma- and X-ray photons because most of them require sufficiently intense coherent control fields, which are yet inaccessible in this range.

Alternative methods for the delay of photons, which are based on the decrease in their velocity in a nuclear medium in the presence of the Mössbauer

effect were demonstrated in the gamma- and X-ray regions. An effect that is similar to the electromagnetically induced transparency and is accompanied by the delay of 14.4-keV photons was observed in a $FeCO_3$ crystal due to the approach of the energy sublevels of the excited state of ^{57}Fe nuclei at a crystal temperature of 30 K [38]. The decrease in the velocity of 14.4-keV photons emitted by the ^{57}Co radioactive source was observed at room temperature in a number of chemical compounds whose composition provides a doublet structure and sharp dispersion of a resonance quantum transition in the included ^{57}Fe nuclei [39]. The controlled delay of spectrally narrow X-ray pulses with a photon energy of 14.4 keV propagating in a cavity containing a nanolayer of ^{57}Fe nuclei was observed in [40]. The possibility of the controlled decrease in the velocity of 14.4-keV photons in the ^{57}Fe absorber due to the acoustically induced transparency (AIT), which appears at collective vibrations of atomic nuclei with certain amplitude and frequency, was demonstrated in [37, 41, 42].

Furthermore, the possibility of localization of a single-photon wave packet with a photon energy of 14.4 keV in the medium of ^{57}Fe nuclei followed by the subsequent coherent on-demand extraction of a fraction of the field resonantly absorbed by ^{57}Fe nuclei in the form of short gamma-ray pulses has been demonstrated in [43–49]. In experiments with the ^{57}Co radioactive source, a short pulse appeared at the sharp displacement of the source [43, 44] or the ^{57}Fe absorber [45, 46] by a distance of about the photon wavelength due to the displacement-induced constructive interference between the incident and coherently scattered fields. The effect is called gamma echo. The gamma radiation from the $^{57}FeBO_3$ crystal emitted after the passage of a synchrotron pulse through it was similarly suppressed by means of the sharp change in the direction of magnetization, which induced the destructive interference between the spectral polarization components of ^{57}Fe nuclei. The subsequent on-demand restoration of the initial direction of magnetization induced a short radiation burst similar to gamma echo [47]. Short bursts against the background of the gradually decreasing intensity of the single-photon wave packet were observed at the output of the oscillating ^{57}Fe absorber after the passage of synchrotron radiation [48, 49] and radiation from the ^{57}Co radioactive source [36, 50] through it due to the Doppler transformation of the singlet spectral line of the absorber to the phased comb of spectral lines similar to an atomic frequency comb in the optical region.

The authors of [51] theoretically proposed a method for implementing nuclear quantum memory for 14.4-keV photons, which was based on a sequence of several resonant ^{57}Fe absorbers moving at different constant velocities along the propagation direction of a spectrally narrow synchrotron pulse. Due to the

Doppler effect, the absorption spectral lines of moving absorbers are shifted with respect to each other, forming a spectral comb similar to an atomic frequency comb. The frequencies of the comb teeth are determined by the magnitudes and directions of the velocities of the absorbers, similar to the gradient photon echo method, allowing one to reconstruct on demand the initial X-ray pulse.

It is noteworthy that both the propagation of photons at any frequency in the medium and their localization are the result of the annihilation of a photon interacting with an atom (nucleus) and the subsequent creation of another photon emitted by this or another atom (nucleus). In this case, the characteristics of the passed photon are determined by the characteristics of incident photons and particles of the medium, as well as by the conditions of their interaction.

In this work, a method for on-demand reconstruction of an arbitrary part of the initial photon wave packet absorbed by ^{57}Fe nuclei is proposed on an example of 14.4-keV gamma-ray photons emitted by the ^{57}Co radionuclide. Unlike the above methods for the dispersive delay of gamma- and X-ray photons and for the extraction on demand of a part of gamma/X rays absorbed by the medium, this method allows one to reconstruct with delay the initial spectral–temporal characteristics of the single-photon wave packet with a Lorentzian spectrum by the control of the transmittance of the resonantly absorbed medium via AIT. Experimental conditions for the implementation of this method are proposed. The physical mechanism of the effect and its correspondence to the quantum memory mechanism, as well as the possibility of implementing the time-resolved Mössbauer spectroscopy of materials for the first time, are discussed.

2. SINGLE-PHOTON WAVE PACKET

The waveform of a 14.4-keV photon is usually measured by the delay coincidence method (see Fig. 1), which is as follows. First, the time of detection of a 122-keV photon is determined, which indicates the transition of one of the ^{57}Co nuclei in the source to the excited energy level $|b\rangle$ (see the left inset of Fig. 1) and possibility of emitting the 14.4-keV photon. The detector sends a 122-keV Start measure signal to switch on a unit for the detection of the 14.4-keV photon. Then, the time interval to the detection of the 14.4-keV photon, i.e., the time interval between the appearance of the possibility of emitting the 14.4-keV photon by the nucleus and its detection, is measured. This procedure is repeated many times. As a result, the dependence of the number of detected 14.4-keV photons on the time from the appearance of the possibility of emitting each photon by the source is obtained. It is proportional to the dependence of the probability of detecting one 14.4-keV photon on the time from the appearance of the possibility of its emission by the
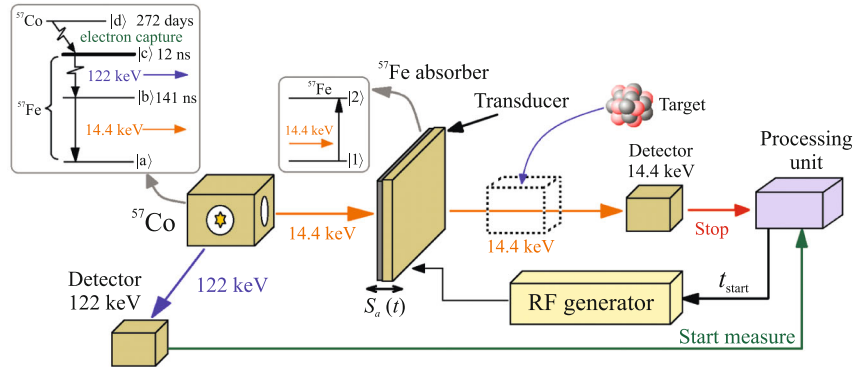
Fig. 1. (Color online) General delayed coincidence scheme to count the number of consecutive detected 122- and 14.4-keV photons. The multiply measured interval between the Start measure (generated by the 122-keV detector) and Stop (generated by the 14.4-keV detector) signals gives the frequency of coincidence counts as a function of the delay of a 14.4-keV photon with respect to a 122-keV photon, which is proportional to the time dependence of the probability of detecting the 14.4-keV photon or, equivalently, to the waveform of the photon. The left and right insets show the energy diagrams of the ^{57}Co source and the ^{57}Fe absorber, respectively. The quantum transition frequency of the source in the proposed method is tuned to the quantum transition frequency of the absorber, which is a stainless steel foil containing the ^{57}Fe Mössbauer nuclide. The foil is attached to a piezoelectric transducer, whose harmonic vibrations begin at a certain time t_{start} after the detection of the 122-keV photon. The studied material Target containing the ^{57}Fe Mössbauer nuclide should be placed in a box marked by dotted lines for time-resolved Mössbauer spectroscopy.

source. The entire set of detection times of 14.4-keV photons constitutes a single-photon wave packet or a single gamma-ray photon pulse. The mentioned time dependence of the probability of detecting one photon is proportional to the intensity of the single gamma-ray photon pulse and is also called the waveform of the photon, and the time of detecting the 122-keV photon specifies the beginning of the single-photon wave packet with a photon energy of 14.4 keV.

In the laboratory reference frame, the single-photon wave packet that is emitted by the ^{57}Co source and is detected by the 14.4 keV detector can be represented in the form of a quasimonochromatic plane wave whose electric field at the detection point is given by the expression [36−47]

$$E_{in}(t) = E_0\theta(t)\exp(-\gamma t - i\omega_S t), \quad (1)$$

where ω_S and E_0 are the carrier frequency and amplitude of the single-photon wave packet, respectively, and $\gamma \approx 3.6\times10^6$ s^{-1} is the half-width of the spectral line of the corresponding quantum transition in ^{57}Co nuclei. The single gamma-ray photon pulse with the electric field specified by Eq. (1) has a single Lorentzian spectral line.

3. TRANSFORMATION OF SINGLE-PHOTON WAVE PACKET IN THE MÖSSBAUER ABSORBER IN THE REGIME OF ACOUSTICALLY INDUCED TRANSPARENCY

In the proposed experiment, 14.4-keV photons pass through the ^{57}Fe Mössbauer absorber, which is a thin stainless still foil containing ^{57}Fe Mössbauer nuclides

(see Fig. 1). At a certain time t_{start} from the detection time of the 122-keV photon, harmonic vibrations of the absorber along the propagation direction of 14.4-keV photons begins with the constant amplitude R and frequency Ω identical for all nuclei:

$$S_a(t) = R\theta(t - t_{start})\{1 + \sin[\Omega(t - t_{start}) - \pi/2]\}, \quad (2)$$

where $\theta(t)$ is the Heaviside step function. The observation time in Eqs. (1) and (2) is measured from the detection time of the 122-keV photon.

It is convenient to describe the transformation of the single-photon wave packet in the moving resonant absorber in the reference frame of the absorber. In this case, the wave packet given by Eq. (1) is frequency modulated because of the Doppler effect and its electric field has the form [36, 37, 41, 52−54]:

$$E'_{in}(t) = E_0\theta(t)\exp(-\gamma t - i\omega_S t + ip\theta(t - t_{start}) \\ \times \{1 + \sin[\Omega(t - t_{start}) - \pi/2]\}), \quad (3)$$

where $p = 2\pi R/\lambda_S$ is the modulation index at the wavelength $\lambda_S = 0.86$ Å of the 14.4-keV photon.

The electric field of the single-photon wave packet at the output of the absorber at rest in the comoving reference frame can be determined by calculating the convolution of the incident wave packet (3) with the time response function of the absorber $R(t)$ [43, 44, 55]:

$$E'_{out}(t) = \int_{-\infty}^{\infty} R(t - \tau)E'_{in}(\tau)d\tau. \quad (4)$$

Here,

$$R(t) = \delta(t) - \frac{T_a\gamma}{2}\theta(t)e^{-(i\omega_a+\gamma)t}\frac{J_1(2\sqrt{T_a\gamma t/2})}{\sqrt{T_a\gamma t/2}}, \quad (5)$$

where $\delta(t)$ is the Dirac delta function; $J_n(p)$ is the nth order Bessel function of the first kind; ω_a and T_a are the frequency of the resonant transition and the Mössbauer (optical) thickness of the absorber, respectively; it is assumed that the spectral lines of the source and the absorber have the same width $\gamma_a = \gamma$; and the nonresonant absorption of the field due to the photoelectric effect is disregarded because it is not measured in the proposed experiment.

Substituting Eqs. (3) and (5) into Eq. (4) and taking into account the condition of resonance between the source at rest and the absorber $\omega_S = \omega_a = \omega_{res}$, we obtain

$$E'_{out}(t) = E_0\theta(t)e^{-(i\omega_{res}+\gamma)t}$$

$$\times\left[e^{ip\theta(t-t_{start})\{1+\sin[\Omega(t-t_{start})-\pi/2]\}} - \frac{T_a\gamma}{2}\right.$$

$$\times\int_0^t\frac{J_1(2\sqrt{T_a\gamma(t-\tau)/2})}{\sqrt{T_a\gamma(t-\tau)/2}} \quad (6)$$

$$\left.\times e^{ip\theta(\tau-t_{start})\{1+\sin[\Omega(\tau-t_{start})-\pi/2]\}}d\tau\right].$$

According to Eq. (6), the field at the output of the absorber at any time can be represented as the sum of the field at the input of the absorber (the first term in Eq. (6)) and the coherently forward scattered field (the second term in Eq. (6)), which corresponds to the induced nuclear polarization [43, 44, 55]. At $0 \le t \le t_{start}$, when the absorber is at rest, the interference of these fields destroys the single-photon pulse incident on the absorber. As a result, according to Eq. (6), the field of the single-photon wave packet at the output of the absorber takes the form

$$E'_{out}(t) = E_0\theta(t)J_0(\sqrt{2T_a\gamma t})e^{-(i\omega_{res}+\gamma)t}. \quad (7)$$

After the beginning of acoustical vibrations, the field at $t \ge t_{start}$ can be represented as

$$E'_{out}(t) = E_0\theta(t)e^{-i\omega_{res}+\gamma)t}$$

$$\times\left[e^{ip\theta(t-t_{start})\{1+\sin[\Omega(t-t_{start})-\pi/2]\}} - \frac{T_a\gamma}{2}\right.$$

$$\times\int_0^{t_{start}}\frac{J_1(2\sqrt{T_a\gamma(t-\tau)/2})}{\sqrt{T_a\gamma(t-\tau)/2}}d\tau - \frac{T_a\gamma}{2} \quad (8)$$

$$\left.\times e^{ip}\int_{t_{start}}^t\frac{J_1(2\sqrt{T_a\gamma(t-\tau)/2})}{\sqrt{T_a\gamma(t-\tau)/2}}e^{ip\sin[\Omega(\tau-t_{start})-\pi/2]}d\tau\right].$$

We consider the case where the absorber vibrates in the regime of AIT [37, 41, 42] under the conditions

$$\begin{aligned} J_0(p) &= 0, \\ T_a\gamma/\Omega &\ll 1. \end{aligned} \quad (9)$$

The first condition is satisfied, e.g., at the amplitude of vibrations of the absorber $R \approx 0.38\lambda_S$, which corresponds to the modulation index $p \approx 2.4$. In this case, the integrals in Eq. (8) have analytical representations, and the electric field of the single-photon wave packet at the output of the absorber in the comoving reference frame is represented in the form

$$E'_{out}(t) = E_0\theta(t)e^{-(i\omega_{res}+\gamma)t}$$

$$\times\begin{cases} J_0(\sqrt{2T_a\gamma t}), & t \le t_{start}, \\ e^{ip\{1+\sin[\Omega(t-t_{start})-\pi/2]\}} + [J_0(\sqrt{2T_a\gamma t}) \\ - J_0(\sqrt{2T_a\gamma(t-t_{start})})], & t \ge t_{start}. \end{cases} \quad (10)$$

To pass to the laboratory reference frame, it is necessary to multiply Eq. (10) by $\exp[-i2\pi S_a(t)/\lambda_S]$ [36, 37, 41, 52–54]:

$$E_{out}(t) = E_0\theta(t)e^{-(i\omega_{res}+\gamma)t}$$

$$\times\begin{cases} J_0(\sqrt{2T_a\gamma t}), & t \le t_{start}, \\ 1 + [J_0(\sqrt{2T_a\gamma t}) - J_0(\sqrt{2T_a\gamma(t-t_{start})})] \\ \times e^{-ip}\sum_{n=-\infty}^{\infty} J_n(p)e^{-in\Omega(t-t_{start})+in\pi/2} & t \ge t_{start}, \end{cases} \quad (11)$$

where the Jacobi–Anger relation $e^{\pm ip\sin\phi} = \sum_{n=-\infty}^{\infty} J_n(p)e^{\pm in\phi}$ is used and it is taken into account that $J_0(p) = 0$ according to Eqs. (9).

4. ON-DEMAND RECONSTRUCTION OF A PART OF THE SINGLE-PHOTON PULSE

It follows from Eq. (11) that the single-photon wave packet, which is emitted by the ^{57}Co source, is absorbed resonantly in the medium of ^{57}Fe nuclei in the time interval $0 \le t \le t_{start}$, when the absorber is at rest with respect to the source. Consequently, its envelope no longer has the initial exponential shape, and the spectral line is no longer Lorentzian but remains single.

After the beginning of vibrations of the absorber in the regime of AIT under conditions (9) at $t \ge t_{start}$, the single-photon wave packet at the output of the medium becomes multicomponent; i.e., it consists of several spectral lines. More precisely, according to the second term in the part of Eq. (11) referring to $t \ge t_{start}$, the spectral lines at frequencies $\omega_{res} + n\Omega$ separating from the spectral line of the incident field by an integer number of the frequencies of vibrations of the absorber with
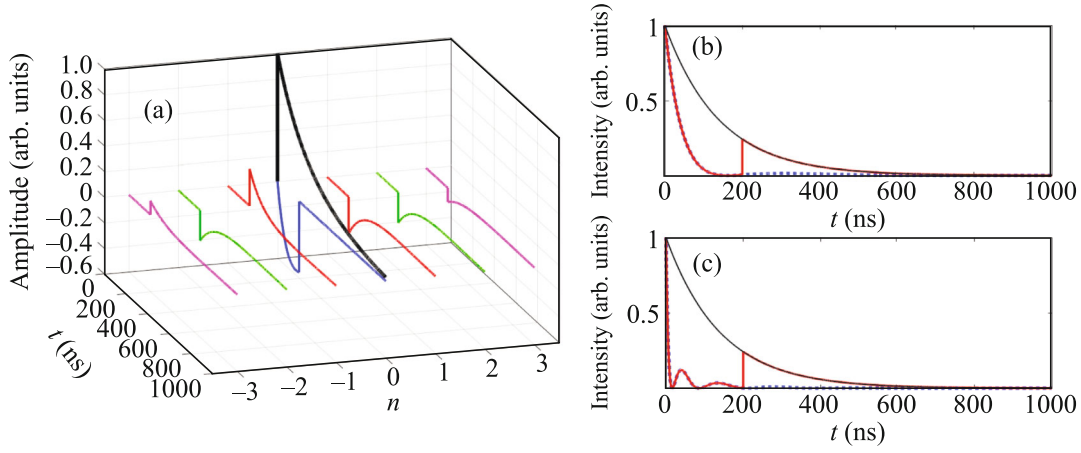
Fig. 2. (Color online) (a) Time dependences of (black line) the incident field amplitude appearing in Eq. (1) at the carrier frequency ω_{res} and frequency components of the coherently scattered field given by Eq. (11) at the frequencies $\omega_{res} + n\Omega$ including the sign of $J_n(p)$ (blue, red, green, and violet lines) at the output of the resonant nuclear absorber with an optical thickness of $T_a = 5$, which begins to oscillate according to Eq. (2) in the regime of acoustically induced transparency ($p = 2.41$, $\Omega/(2\pi) = 100$ MHz) at the time $t_{start} = 200$ ns. The red solid line in panels (b, c) is the waveform of the 14.4-keV photon at the output of the absorber, which moves according to Eq. (2), that is specified by Eq. (12), is detected by a relatively narrowband detector, and is "sensed" by the target indicated as Target in Fig. 1. The optical thickness of the absorber is $T_a = $ (b) 5 and (c) 50. The black thin solid line in (b, c) is the waveform the photon at the input of the absorber and the blue dashed line in (b, c) is the waveform of the photon at the output of the absorber of the same optical thickness at rest.

the amplitudes $J_n(p)[J_0(\sqrt{2T_a\gamma t}) - J_0(\sqrt{2T_a\gamma(t - t_{start})})]$ and the corresponding phases appear in the spectrum of the output field (see Fig. 2a). According to Eqs. (9), the interval between the spectral lines is much wider than the spectral width of the initial single-photon pulse.

At the same time, according to Eqs. (9), the output field near the carrier frequency of the initial single-photon wave packet at $t \geq t_{start}$ is described by only the first term in the part of Eq. (11) referring to $t \geq t_{start}$. In other words, after the beginning vibrations of the absorber at the arbitrary time t_{start}, the field of the photon with the carrier frequency ω_{res} passed through the absorber takes the form $E_{out}(t) = E_0\theta(t)e^{-(i\omega_{res}+\gamma)t}$ ($t > t_{start}$). Thus, both the exponential shape of the envelope and the corresponding Lorentzian contour of the spectral line of the initial single-photon pulse are reconstructed. Only the peak amplitude of the pulse determined by the time t_{start} decreases as $E_{out}^{max}(t) = E_0 e^{-\gamma t_{start}}$. In this case, according to Eq. (11), the intensity of the single-photon pulse $I_{out}(t) = c|E_{out}(t)|^2/(8\pi)$ measured by the relatively narrowband detector with the width of the detection spectral line $\gamma \ll \Delta\omega_{det} \ll \Omega$ has the form (see Figs. 2b and 2c)

$$I_{out}(t)|_{\gamma \ll \Delta\omega_{det} \ll \Omega} = I_0\theta(t)e^{-2\gamma t}\begin{cases} J_0^2(\sqrt{2T_a\gamma t}), & t \leq t_{start}, \\ 1, & t \geq t_{start}, \end{cases} \quad (12)$$

where $I_0 = cE_0^2/(8\pi)$.

5. RECONSTRUCTION OF THE PART OF THE SINGLE-PHOTON PULSE AND QUANTUM MEMORY

The considered process of the resonance conversion of the energy of the single-photon wave packet into the polarization of nuclei, the destruction of the initial single-photon wave packet and the localization of the electromagnetic field in the absorber at $0 \leq t \leq t_{start}$ are explained by the excitation of the antiphase nuclear polarization of the absorber at the frequencies of the incident field (blue line in Fig. 2a), which destructively interferes with the field exciting this polarization (black line in Fig. 2a). Due to the vibrations of the absorber that begin at the time t_{start} and satisfy the AIT conditions specified by Eqs. (9), the polarization of nuclei in the absorber begins to evolve at frequencies significantly different from the frequencies of the exciting field, whereas the previously induced polarization at the frequencies of the spectral line of the incident field vanishes. In this case, the resonant absorber becomes transparent; i.e., the polarization at the frequencies of the field is no longer excited and no longer suppresses the propagating field. As a result, the field with the initial spectral–temporal characteristics, as well as the coherently scattered field at frequencies far from the spectral line of the incident field, appear at the output of the absorber at $t \geq t_{start}$. In other words, the spectral separation of the incident field and the polarization of the absorber occurs and results in the reconstruction of the part of the single-photon pulse corresponding to the time $t \geq t_{start}$. Thus,

the part of the single-photon pulse is reconstructed on demand by means of the controlled transmittance of the resonant absorber.

It is seen in Eqs. (11) and (12) that, in the case of the ^{57}Co source with the Lorentzian spectral line, the reconstructed part of the single-photon wave packet specified by Eq. (1) differs from the initial wave packet only in the peak amplitude determined by the arbitrary time t_{start}. The time t_{start} can in turn be much longer than the characteristic FWHM of the single-photon pulse $\tau = \ln2/(2\gamma) \approx 98$ ns (see Fig. 2b with $t_{start} = 200$ ns). Thus, the part of the single-photon pulse with the Lorentzian contour reconstructed by this method formally satisfies the criteria for delay of the photon by means of quantum-optical memory [19−35, 51].

At the same time, the proposed method is based on a physical mechanism fundamentally different from the mechanism of the above quantum-optical memory methods [19−35, 51]. The quantum memory methods are based on the transformation of the electromagnetic field into a certain quantum state of atoms or nuclei of the medium that is characterized by coherence (or the polarization in the case of allowed quantum transitions). The incident-pulse-induced coherence (polarization) evolves during a certain time after the electromagnetic field of the pulse vanishes in the medium. In other words, the field and the coherence of the medium induced by it are separated in time. Due to this time separation, most of the quantum-optical memory methods make it possible to delay the pulse by a time exceeding its total duration measured from the pulse formation time to its disappearance time. At the same time, the spectral−temporal characteristics of the field after the inverse conversion of the atomic (nuclear) coherence (polarization) into the field are determined by the properties of the corresponding quantum transitions of atoms (nuclei), by the interaction of the field with the medium, and by the procedure of extraction of the field from the medium [19−35, 51].

The proposed method is based on the separation of the spectral lines of the incident field and the polarization of absorbing nuclei in order to exclude their overlapping. This spectral separation at the time t_{start} removes the interaction of the field with the medium. As a result, the nuclear polarization is no longer excited at the frequencies of the incident field; therefore, a part of the initial single-photon pulse corresponding to the time $t \geq t_{start}$ passes through the absorber without change in its characteristics. In other words, the reconstruction of a part of the initial wave packet is in fact the "cutoff" of its leading part due to resonant absorption in the medium and the undisturbed passage of the remaining part that does not interact with the medium. This method allows one to "delay" a part of the single-photon pulse only by a time no longer than its total duration measured from the pulse formation time to its disappearance time. In

addition, the front of the delayed part of pulses with a non-Lorentzian spectrum will differ from the envelope of the initial pulse.

This method of "delayed transmission" of the part of the single-photon wave packet with the Lorentzian spectrum is similar to gamma-echo effects [43−46] because it is also based on the control of the interference interaction between the initial field and the polarization of the absorber. However, the fast displacement of the absorber with respect to the source in the case of gamma echo changes the phase difference between the incident and coherently scattered fields without change in their frequencies. In our case, after the beginning of vibrations of the absorber, the nuclear polarization vanishes at all frequencies of the incident field and appears at frequencies far from the spectrum of the incident field. Consequently, this method can be considered as a combination of acoustically induced transparency [41, 54] and gamma echo [43−46].

6. TIME-RESOLVED MÖSSBAUER SPECTROSCOPY

The described method for the on-demand reconstruction of the single-photon wave packet with a photon energy of 14.4 keV emitted by the ^{57}Co radioactive source can significantly expand the capabilities of the known Mössbauer nuclear spectroscopy methods [56] by providing time-resolved spectroscopic measurements. Indeed, if the test target doped with ^{57}Fe nuclei is placed behind the absorber, only the part of the single-photon pulse reconstructed at the time t_{start} will efficiently interact with ^{57}Fe nuclei of the target due to vibrations of the absorber (see Fig. 1). In other words, the interaction of 14.4-keV photons with ^{57}Fe nuclei of the target in this case will be delayed by the time t_{start}. It is implied that the studied dynamic process in the target begins at the time of detection of the 122-keV photon. Thus, if there are some processes changing the states of ^{57}Fe nuclei, both the waveform and spectrum of the photon at the output of the target will depend on the delay time t_{start}, reflecting the dynamics of internal processes in the medium.

It is noteworthy that the idea of the delayed single-photon pulse, which underlies the proposed method for time-resolved probing of the state of nuclei in the target, can also be implemented in the absence of the absorber forming the two-pulse waveform of the 14.4-keV photon. To this end, the detection time of the 122-keV photon in each measurement event will determine the time t_{start} with respect to the beginning of the dynamic process in the target, which is used in this case as the onset of the time scale $t = 0$. At the same time, the corresponding single-photon pulse delayed by the time t_{start} with respect to the beginning of the studied dynamic process in the target will be formed at the time of the subsequent detection of the 14.4-keV
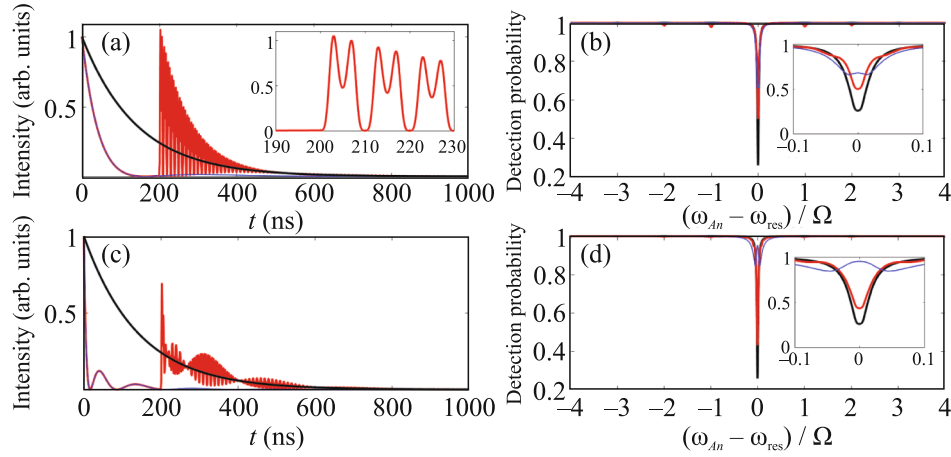
Fig. 3. (Color online) Waveform of the 14.4-keV photon given by Eq. (13) (red line) at the output of the absorber with the optical thickness T_a = (a) 5 and (c) 50, which begins to oscillate according to Eq. (2) in the regime of acoustically induced transparency ($p = 2.41$, $\Omega/(2\pi) = 100$ MHz) at the time $t_{start} = 200$ ns, (black line) at the input of the medium, and (thin blue line) at the output of the same absorber at rest. (b, d) Corresponding spectra of the detection probability of the 14.4 keV photon (red line) passed through the absorber moving according to Eq. (2), (thin blue line) passed through the absorber at rest, and (black line) in the absence of the absorber; lines are results of the simulation of change in the spectrum of the 14.4-keV photon passed through the absorber by the method described in [57] using the absorber analyzer with the optical thickness $T_a^{(An)} = 5$.

photon by the delayed coincidence method. The multiple repetition of this procedure forms a set of waveforms of the 14.4-keV photon, which depend on the time interval t_{start} from the beginning of the dynamic process in the target. A more detailed discussion and comparison of these methods of the time-resolved Mössbauer diagnostics of dynamic processes are beyond the scope of this work and will be reported in next works.

7. INTERFERENCE OF THE NUCLEAR POLARIZATION AND THE INCIDENT FIELD

We discuss the experiment where 14.4-keV photons are detected by a broadband detector covering the entire frequency range generated by the vibrating absorber and the test medium is absent. In this case, after the beginning of vibrations of the absorber, the detector at $t \geq t_{start}$ will detect the interference of the field of the reconstructed single-photon pulse with the multicomponent field of the induced nuclear polarization, which has the form of repeated bursts (see Fig. 3). According to Eq. (11), the detected intensity of the single-photon pulse passed through the absorber has the form

$$I_{out}(t) = I_0\theta(t)e^{-2\gamma t}$$

$$\times \begin{cases} J_0^2(\sqrt{2T_a\gamma t}), & t \leq t_{start}, \\ 1 + [J_0(\sqrt{2T_a\gamma t}) - J_0(\sqrt{2T_a\gamma(t - t_{start})})]^2 \\ + 2[J_0(\sqrt{2T_a\gamma t}) - J_0(\sqrt{2T_a\gamma(t - t_{start})})] \\ \times \cos[p + p\sin[\Omega(t - t_{start}) - \pi/2]], & t \geq t_{start}, \end{cases} \quad (13)$$

where the last term of the sum describes interference bursts at $t \geq t_{start}$.

As follows from Eq. (13) and seen in Fig. 3, the nuclear polarization, being spectrally separated from the incident field at the time t_{start}, no longer suppresses this field. However, in contrast to the case of a narrowband detector, which detects only photons near the spectral line of the incident single-photon pulse, the detection of photons at all frequencies of the coherently scattered field reveals the time-dependent interference between the field of the multicomponent nuclear polarization and the incident single-photon pulse. The change in the waveform of the passed photon with increasing optical thickness of the absorber is due to a large resonant absorption of the coherently scattered field at the frequencies of its spectral components (see Fig. 3c). In this case, both the time profile of the intensity (see Figs. 2b and 2c) and the spectral profile of the field passed through the absorber near the spectral line of the incident single-photon pulse remain almost unchanged (see Figs. 3b and 3d). Insignificant broadening and distortion of the spectral profile of the single-photon pulse at the output of the absorber with increasing optical thickness of the absorber (cf. red lines in Figs. 3d and Fig. 3b) are due to the stronger attenuation of the field before the beginning of vibrations, whereas after the beginning of vibrations, the resonant absorber becomes transparent in both cases because of the satisfaction of the AIT conditions (9).

Similar to the detection of photons by the narrowband detector considered above, the waveforms of the photon shown in Fig. 3 can also be used for time-

resolved spectroscopic measurements because the interaction of the single-photon pulse with the tested medium in both cases changes only a part of the single-photon wave packet that corresponds to the initial single-photon pulse. In this case, deterministic oscillations of the intensity caused by the induced nuclear polarization at strongly different frequencies can increase the information capability of the method in cases where these frequencies approach the frequencies of some quantum transitions in nuclei of the tested medium. If resonances at the frequencies of the induced nuclear polarization are absent in the medium, the corresponding oscillations of the intensity of the single-photon wave packet can be filtered when processing the results of measurements.

8. CONCLUSIONS

To summarize, a method has been proposed to reconstruct on demand a single-photon wave packet with a Lorentzian spectrum and a photon energy of 14.4 keV resonantly absorbed in the medium of ^{57}Fe nuclei. The method is based on the frequency discrimination of the field propagating in the absorber and resonance nuclear polarization induced by this field in the presence of delayed acoustically induced transparency in the absorber. The frequency discrimination has been implemented through the Doppler effect; to this end, the acoustic vibrations of the absorber at certain frequency and amplitude ensuring conditions for acoustically induced transparency are switched on at an arbitrary time. Similarities and differences of the proposed method and the known quantum-optical memory methods and methods of nuclear polarization control in the gamma range have been revealed. It has been shown that this method allows the implementation of the time-resolved Mössbauer spectroscopy of various media.

ACKNOWLEDGMENTS

We are grateful to O.A. Kocharovskaya for stimulating discussion.

FUNDING

This work was supported by the Ministry of Science and Higher Education of the Russian Federation, agreement no. 075-15-2022-316 with the Center of Excellence "Center of Photonics."

CONFLICT OF INTEREST

The authors of this work declare that they have no conflicts of interest.

REFERENCES

1. A. Kasapi, M. Jain, G. Y. Yin, and S. E. Harris, Phys. Rev. Lett. **74**, 2447 (1995).
2. L. V. Hau, S. E. Harris, Z. Dutton, and C. H. Behroozi, Nature (London, U.K.) **397**, 594 (1999).
3. D. Budker, D. Kimball, S. Rochester, and V. Yashchuk, Phys. Rev. Lett. **83**, 1767 (1999).
4. M. M. Kash, V. A. Sautenkov, A. S. Zibrov, L. Hollberg, G. R. Welch, M. D. Lukin, Y. Rostovtsev, E. S. Fry, and M. O. Scully, Phys. Rev. Lett. **82**, 5229 (1999).
5. A. V. Turukhin, V. S. Sudarshanam, M. S. Shahriar, J. A. Musser, B. S. Ham, and P. R. Hemmer, Phys. Rev. Lett. **88**, 023602 (2002).
6. M. S. Bigelow, N. N. Lepeshkin, and R. W. Boyd, Phys. Rev. Lett. **90**, 113903 (2003).
7. M. S. Bigelow, N. N. Lepeshkin, and R. W. Boyd, Science (Washington, DC, U. S.) **301**, 200 (2003).
8. A. H. Safavi-Naeini, T. P. Mayer Alegre, J. Chan, M. Eichenfield, M. Winger, Q. Lin, J. T. Hill, D. E. Chang, and O. Painter, Nature (London, U.K.) **472**, 69 (2011).
9. H. Xionga and Y. Wu, Appl. Phys. Rev. **5**, 031305 (2018).
10. E. Saglamyurek, T. Hrushevskyi, A. Rastogi, K. Heshami, and L. J. Le Blanc, Nat. Photon. **12**, 774 (2018).
11. A. Rastogi, E. Saglamyurek, T. Hrushevskyi, S. Hubele, and L. J. Le Blanc, Phys. Rev. A **100**, 012314 (2019).
12. M. F. Yanik, W. Suh, Zh. Wang, and Sh. Fan, Phys. Rev. Lett. **93**, 233903 (2004).
13. Y. Okawachi, M. A. Foster, J. E. Sharping, A. L. Gaeta, Q. Xu, and M. Lipson, Opt. Express **14**, 2317 (2006).
14. T. Wang, Y.-Q. Hu, Ch.-G. Du, and G.-L. Long, Opt. Express **27**, 7344 (2019).
15. R. Y. M. Manjappa, Y. K. Srivastava, and R. Singh, Appl. Phys. Lett. **111**, 021101 (2017).
16. Zh. Zhao, H. Zhao, R. T. Ako, J. Zhang, H. Zhao, and Sh. Sriram, Opt. Express **27**, 26459 (2019).
17. O. Kocharovskaya and Ya. I. Khanin, Sov. Phys. JETP **63**, 945 (1986).

18. K. J. Boller, A. Imamoğlu, and S. E. Harris, Phys. Rev. Lett. **66**, 2593 (1991).

19. A. I. Lvovsky, B. C. Sanders, and W. Tittel, Nat. Photon. **3**, 706 (2009).

20. M. Afzelius, N. Gisin, and H. de Riedmatten, Phys. Today **68** (12), 42 (2015).

21. T. Chaneliére, D. N. Matsukevich, S. D. Jenkins, S.-Y. Lan, T. A. B. Kennedy, and A. Kuzmich, Nature (London, U. K.) **438**, 833 (2005).

22. J. J. Longdell, E. Fraval, M. J. Sellars, and N. B. Manson, Phys. Rev. Lett. **95**, 63601 (2005).

23. K. F. Reim, J. Nunn, V. O. Lorenz, B. J. Sussman, K. C. Lee, N. K. Langford, D. Jaksch, and I. A. Walmsley, Nat. Photon. **4**, 218 (2010).

24. K. F. Reim, P. Michelberger, K. C. Lee, J. Nunn, N. K. Langford, and I. A. Walmsley, Phys. Rev. Lett. **107**, 053603 (2011).

25. K. Reim, J. Nunn, X.-M. Jin, P. Michelberger, T. Champion, D. England, K. Lee, W. Kolthammer, N. Langford, and I. Walmsley, Phys. Rev. Lett. **108**, 263602 (2012).

26. M. Afzelius, C. Simon, H. de Riedmatten, and N. Gisin, Phys. Rev. A **79**, 052329 (2009).

27. C. Clausen, I. Usmani, F. Bussieres, N. Sangouard, M. Afzelius, H. de Riedmatten, and N. Gisin, Nature (London, U.K.) **469**, 508 (2011).

28. E. Saglamyurek, N. Sinclair, J. Jin, J. Slater, D. Oblak, F. Bussieres, M. George, R. Ricken, W. Sohler, and W. Tittel, Phys. Rev. Lett. **108**, 083602 (2012).

29. M. K. Kim and R. Kachru, Opt. Lett. **14**, 423 (1989).

30. D. L. McAuslan, P. M. Ledingham, W. R. Naylor, S. E. Beavan, M. P. Hedges, M. J. Sellars, and J. J. Longdell, Phys. Rev. A **84**, 022309 (2011).

31. V. Damon, M. Bonarota, A. Louchet-Chauvet, T. Chaneliere, and J.-L. Le Gouet, New J. Phys. **13**, 093031 (2011).

32. S. A. Moiseev and S. Kroll, Phys. Rev. Lett. **87**, 173601 (2001).

33. G. Hetet, M. Hosseini, B. M. Sparkes, D. Oblak, P. K. Lam, and B. C. Buchler, Opt. Lett. **33**, 2323 (2008).

34. G. Hetet, J. J. Longdell, A. L. Alexander, P. K. Lam, and M. J. Sellars, Phys. Rev. Lett. **100**, 23601 (2008).

35. G. Hetet, M. Hosseini, B. M. Sparkes, D. Oblak, P. K. Lam, and B. C. Buchler, Opt. Lett. **33**, 2323 (2008).

36. F. Vagizov, V. Antonov, Y. V. Radeonychev, R. N. Shakhmuratov, and O. Kocharovskaya, Nature (London, U.K.) **508**, 80 (2014).

37. I. R. Khairulin, Y. V. Radeonychev, and O. Kocharovskaya, Sci. Rep. **12**, 20270 (2022).

38. R. Coussement, Y. Rostovtsev, J. Odeurs, G. Neyens, H. Muramatsu, S. Gheysen, R. Callens, K. Vyvey, G. Kozyreff, P. Mandel, R. Shakhmuratov, and O. Kocharovskaya, Phys. Rev. Lett. **89**, 107601 (2002).

39. R. N. Shakhmuratov, F. G. Vagizov, J. Odeurs, M. O. Scully, and O. Kocharovskaya, Phys. Rev. A **80**, 063805 (2009).

40. K. P. Heeg, J. Haber, D. Schumacher, L. Bocklage, H.-C. Wille, K. S. Schulze, R. Loetzsch, I. Uschmann, G. G. Paulus, R. Rüffer, R. Rohlsberger, and J. Evers, Phys. Rev. Lett. **114**, 203601 (2015).

41. Y. V. Radeonychev, I. R. Khairulin, and F. G. Vagizov, Phys. Rev. Lett. **124**, 163602 (2020).

42. Y. V. Radeonychev, I. R. Khairulin, and O. Kocharovskaya, JETP Lett. **114**, 729 (2021).

43. P. Helisto, I. Tittonen, M. Lippmaa, and T. Katila, Phys. Rev. Lett. **66**, 2037 (1991).

44. I. Tittonen, M. Lippmaa, P. Helisto, and T. Katila, Phys. Rev. B **47**, 7840 (1993).

45. R. N. Shakhmuratov, F. G. Vagizov, and O. Kocharovskaya, Phys. Rev. A **84**, 043820 (2011).

46. R. N. Shakhmuratov, F. G. Vagizov, and O. Kocharovskaya, Phys. Rev. A **87**, 013807 (2013).

47. Yu. V. Shvyd'ko, T. Hertrich, U. van Bürck, E. Gerdau, O. Leupold, J. Metge, H. D. Ruter, S. Schwendy, G. V. Smirnov, W. Potzel, and P. Schindelmann, Phys. Rev. Lett. **77**, 3232 (1996).

48. G. V. Smirnov, U. van Burck, J. Arthur, S. L. Popov, A. Q. R. Baron, A. I. Chumakov, S. L. Ruby, W. Potzel, and G. S. Brown, Phys. Rev. Lett. **77**, 183 (1996).

49. G. V. Smirnov and W. Potzel, Hyperfine Interact. **123–124**, 633 (1999).

50. R. N. Shakhmuratov, F. G. Vagizov, V. A. Antonov, Y. V. Radeonychev, M. O. Scully, and O. Kocharovskaya, Phys. Rev. A **92**, 023836 (2015).

51. X. Zhang, W.-T. Liao, A. Kalachev, R. N. Shakhmuratov, M. O. Scully, and O. Kocharovskaya, Phys. Rev. Lett. **123**, 250504 (2019).

52. V. A. Antonov, Y. V. Radeonychev, and O. Kocharovskaya, Phys. Rev. A **92**, 023841 (2015).

53. I. R. Khairulin, V. A. Antonov, Y. V. Radeonychev, and O. Kocharovskaya, Phys. Rev. A **98**, 043860 (2018).

54. I. R. Khairulin, Y. V. Radeonychev, V. A. Antonov, and O. Kocharovskaya, Sci. Rep. **11**, 7930 (2021).

55. G. V. Smirnov, Hyperfine Interact. **123–124**, 31 (1999).

56. *Mössbauer Spectroscopy* Ed. by Yutaka Yoshida and Guido Langouche (Springer, Berlin, 2013). https://doi.org/10.1007/978-3-642-32220-4

57. Supplemental Material. http://link.aps.org/supplemental/10.1103/PhysRevLett.124.163602.

Translated by R. Tyapaev